Measurements of Coulomb Blockade with a Noninvasive Voltage Probe

M. Field, C. G. Smith, M. Pepper,[a] D. A. Ritchie, J. E. F. Frost, G. A. C. Jones, and D. G. Hasko
Cavendish Laboratory, Madingley Road, Cambridge CB3 OHE, United Kingdom
(Received 28 September 1992)

We have investigated the behavior of a laterally confined quantum dot in close proximity to a one-dimensional channel in a separate electrical circuit. When this channel is biased in the tunneling regime the resistance is very sensitive to electric fields, and therefore is sensitive to the potential variations on the dot when it is showing Coulomb blockade oscillations. This effect can be calibrated directly, allowing the Coulomb charging energy to be measured. We also found the activation energy of transport through the dot is much lower than expected.

PACS numbers: 73.20.Dx, 72.15.Nj, 73.40.Gk

Single electron tunneling effects were first identified in granular metal samples [1,2], while later experimental attention focused on submicron metal-oxide-metal tunnel junctions [2], demonstrating that single electron effects can be seen in metal-insulator-metal samples. Lafarge *et al.* [3] measured the potential and hence the charge on the central metallic island of one of these devices by using the known properties of another similar device capacitively coupled in close proximity. A single excess electron on the central island affects the device in the measuring circuit.

Single electron effects have also been observed in semiconductor structures employing "electrostatic squeezing" [4] to vary the shape of an electron gas [5]. The work by Meirav *et al.* [6], and later Kouwenhoven *et al.* [7], demonstrated that the conductance of a lateral quantum dot [8] weakly coupled to connecting leads via tunnel barriers oscillates when the potential is changed on a nearby gate. These oscillations, caused by single electron charging of the quantum dot, have become known as Coulomb blockade (CB) oscillations. It is also probable that earlier transport work on both GaAs and silicon structures can be reinterpreted in terms of charging effects.

In this work we have measured the electrostatic potential of a semiconductor quantum dot showing single electron effects by means of a separate measuring circuit in close proximity. A ballistic one-dimensional channel is used as a "detector" in the other circuit, and we show that it is possible to measure in a noninvasive way the potential on the dot [9] in the regime of CB oscillations.

A diagram of the gate geometry used is shown in the inset to Fig. 1. The gates are fabricated on top of a GaAs/AlGaAs heterostructure with a two-dimensional electron gas (2DEG) 700 Å below the surface of the semiconductor. The ungated 2DEG has a mobility of 120 $m^2V^{-1}s^{-1}$ and a sheet carrier concentration of $(3.61 \pm 0.16) \times 10^{15}\ m^{-2}$. The lithographically defined dimensions of the dot are $0.75 \times 0.34\ \mu m$. Including a depletion width of half the separation of one of the split gate constrictions ($0.1\ \mu m$), we estimate the dot will be approximately $0.65 \times 0.24\ \mu m$. From the behavior of the dot in a magnetic field, we estimate the number of electrons in the dot as $N = 532 \pm 85$ (see below). All experiments were performed in a dilution refrigerator with a base temperature $T < 20$ mK using ac biasing and phase-sensitive detection.

The bar down the middle (G1) separates two electrical circuits which interact via the electric fields present between the regions in close proximity. This gate is biased sufficiently negative that electrons cannot tunnel across; a bias voltage of 0.1 V is required before a current of 1 pA starts to flow. To the right of the bar is a CB structure. An applied ac bias of 10 μV causes current to flow from top to bottom, passing through two constrictions (formed by gates G3 and G5) which help form a quantum dot. The extra gate defining the right-hand edge of the dot

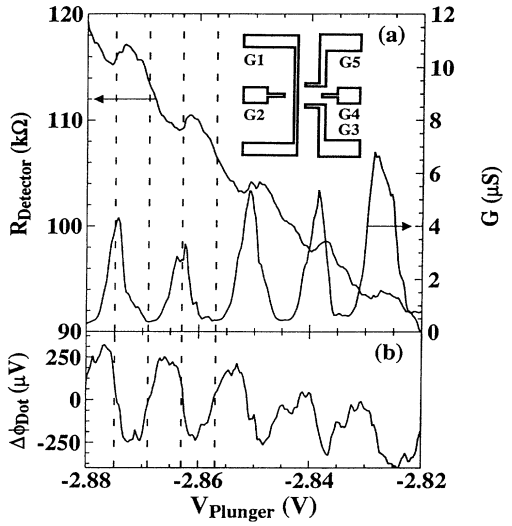

FIG. 1. (a) CB oscillations of conductance vs gate voltage through the dot, together with the resistance of the split gate detector circuit. (b) The change in dot potential calculated from the detector resistance. The overall negative slope is an artifact of the calibration procedure. Inset: a schematic diagram of the gate structure.

(G4) acts as a "plunger." When the voltage on G4 is swept, CB oscillations are seen in the conductance of the quantum dot with a period of 12.28 ± 0.46 mV. The resistance of the channel between G1 and G2 is set at 150 kΩ, where it is most sensitive to the surrounding potential. A constant 1 nA ac current is used in the detector circuit.

Figure 1(a) shows the conductance through the dot and the resistance of the split gate detector as the plunger voltage is swept. The detector resistance has small dips on a rising background which directly correlate with the CB oscillations in the quantum dot. The detector can be calibrated by applying a voltage to the quantum dot region. Using the calibration procedures outlined below, the detector resistance can be transformed into the dot potential as shown in Fig. 1(b). The electrostatic potential of the dot, $\Delta\phi_{\text{dot}}$, is oscillatory with an average amplitude of 500 ± 100 μV, which is therefore the charging energy of the dot. The peaks and troughs of the oscillations in conductance, indicated by the dotted lines, correspond to the mean value of the electrostatic potential oscillations. In a conductance minimum, the Fermi energy in the connecting leads lies approximately midway between the occupied Nth electron state and the inaccessible $(N+1)$th state. As the voltage on the external gate is made more positive, the energy of the occupied electron states in the dot is reduced with respect to the Fermi energy in the connecting leads, i.e., the potential of the dot becomes more positive. When the $(N+1)$th electron level comes within the energy range of the electrons in the leads, electrons can tunnel in. The electron energy levels in the dot move up and down by the charging energy and the measured average electrostatic potential of the dot becomes more negative, reflecting the percentage time an electron is in the dot. The dot potential reflects the difference between the charge on the dot that would minimize the charging energy and the percentage time an extra electron is in the dot. On the conductance peak the dot is occupied 50% of the time by an extra electron and therefore the potential takes the mean value. In between these positions the percentage occupation by an extra electron either lags or leads the charge required causing the oscillation in potential with plunger voltage. In the case of extremely narrow conductance peaks, this can lead to a sawtooth wave form for the dot potential [7].

The charging energy of the dot can also be obtained by measuring the total capacitance of the dot to all other conducting regions around it. CB oscillations have a period in gate voltage of e/C_g, where C_g is the capacitance between the gate being swept and the electrons in the dot [5]. With all the gate voltages set as above, sweeping the potential on each gate a small way allows the capacitance between that gate and the dot to be measured directly. In the same way the capacitance of regions of 2DEG separated from the dot by gates can be measured, e.g., applying a bias to the regions of 2DEG between G4 and G5 and observing the CB oscillations. The capacitances of each conducting region are added up to give the total capacitance $C_\Sigma = (2.92 \pm 0.2) \times 10^{-16}$ F, which implies a potential on the dot due to charging by a single electron $\Delta\phi_{\text{dot}} = e/C_\Sigma = 550 \pm 30$ μV. This is in good agreement with the value obtained from the detector, especially since the calibration is known to underestimate $\Delta\phi_{\text{dot}}$ slightly.

When the temperature is increased the detector resistance variation is washed out at a lower temperature (~ 500 mK) than the conductance oscillations in the box (~ 1.2 K). At this point the thermal fluctuations in the Fermi level around the detector are equal to the shifts in electrostatic potential the detector is measuring. Therefore the detector is seeing a shift in electrostatic potential of $\sim k_B T = 40$ μV, i.e., approximately 8% of the change in electrostatic potential of the dot. This should be equal to the ratio of capacitances $C_{\text{dot-detector}}/C_\Sigma$. The measured ratio using all the 2DEG in the detector circuit is 18%. Estimating the fraction of this due to the 1D channel, by measuring the dot-detector capacitance with the 1D channel present and then pinched off, reduces this ratio to 7%.

The detector is calibrated by removing the plunger (G4) bias and so opening up the far side of the quantum box (see Fig. 1). A voltage can now be applied directly to the 2DEG region between the tunnel barriers of the CB structure and the channel resistance is calibrated as a function of the potential on the quantum box. The leads connected to the dot also float up to the applied voltage and affect the detector. This is, however, a small effect because of the distance of these outer 2DEG regions from the detector [10]. When the plunger (G4) is made increasingly negative the detector tends to pinch off further, picking up the signal from the quantum box on top of a rising background. The correction for the background can be estimated by increasing the temperature until the signal in the detector resistance is no longer observed and subtracting this from the low-temperature data. This corrected curve is the resistance change due to the dot alone, which can then be converted into a dot potential using the calibration described above. Since we are only interested in the change in potential on the dot, the mean potential is then subtracted. In practice a temperature of 1.2 K was sufficient to remove any trace of the signal in the detector resistance.

Relaxing the tunnel barriers slightly so that the conductance G through the dot is $\sim 2e^2/h$ and sweeping either the magnetic field or the plunger voltage shows Aharonov-Bohm-like oscillations in the conductance when the field is such that edge states are formed in the box [11–13]. The period in magnetic flux $\Delta(BA)$ should be h/e, where A is the area of the dot. The measured period in magnetic field is $\Delta B = 20 \pm 2$ mT, giving an active area of $(2.07 \pm 0.20) \times 10^{-13}$ m^2. Using the plunger to change the area of the dot at a constant magnetic field

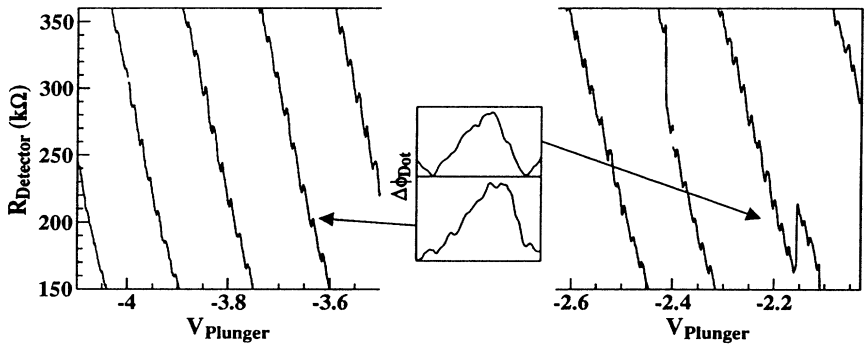

FIG. 2. The detector resistance vs $V_{plunger}$ after the current through the dot has become too small to be measured. The detector resistance is reset to 150 kΩ whenever it reaches 360 kΩ to maintain sensitivity. The resistance curves follow on from each other. The insets show the inferred dot potential at two points; this has changed from the oscillatory shape seen in Fig. 1 to a sawtooth shape.

of 1.285 ± 0.005 T, the Aharonov-Bohm period of oscillation ΔV_{pl}^{AB} was measured to be 105 ± 2 mV. Therefore, $\Delta V_{pl}^{AB}/\Delta A = (3.26 \pm 0.08) \times 10^{13}$ V m^{-2}. Each CB oscillation corresponds to removing one electron from the dot so that $\Delta N/\Delta V_{pl}^{CB}$ the reciprocal of the CB period $= 81.4 \pm 3.2$ V^{-1}. The product of these two values gives the local sheet carrier concentration in the dot $\Delta N/\Delta A = (2.57 \pm 0.16) \times 10^{15}$ m^{-2}. This local value is somewhat lower than the sheet carrier concentration when no gate voltages are applied of $(3.61 \pm 0.16) \times 10^{15}$ m^{-2} obtained from Shubnikov–de Haas oscillations. Combining this value with the area of the dot determined above gives the number of electrons in the dot $N = 532 \pm 85$.

The tunnel barrier heights were increased until the conductance oscillations were only just measurable. The plunger voltage was then swept negative. The conductance oscillations die away because the plunger increases the barrier heights, but the signal on the detector remains. The oscillations of the detector can be followed for a further 110 periods until the plunger reaches a voltage of -4.05 V, after which the signal vanishes (see Fig. 2).

As the oscillations disappear, the background slope of the detector resistance curve becomes much steeper, suggesting that the screening of the plunger by electrons passing through the dot has changed. The current through the dot decreases as the plunger is made more negative and the barrier heights increase. The oscillations should continue until the current decreases to less than one electron through the dot in the time for half a period of the applied ac bias. After this the effective bias is averaged out and the dot behaves like an electron trap, accepting or releasing electrons according to statistical processes.

The dot potential, shown in the insets to Fig. 2, has become a sawtooth wave form. The effective width of the conductance peaks gets smaller and this changes the shape of the potential wave form by reducing the relative width of the peaks with respect to the troughs. The shape continues to change as the plunger is made more negative. The periodicity of the oscillations in plunger voltage gets larger from 16.5 ± 0.3 mV at the low plunger voltages to 19 ± 0.3 mV just before the dot becomes isolated. The increase in period is due to a reduction in the capacitance between the dot and the plunger as the dot gets smaller. The effect is small since the dot still contains over 400 electrons.

Transport in a conductance minimum is by thermal activation of electrons [5] both from the Fermi energy in the connecting leads to the next available state in the dot (activation energy W_1) and from the highest occupied state in the dot to states near the Fermi level in the leads (activation energy W_2). A simple model for the conductance is given by

$$G = G_1 e^{-W_1/kT} + G_2 e^{-W_2/kT}, \quad (1)$$

where $G_{1,2}$ are the conductances through the dot due to the two levels. If the zero-dimensional (0D) level separation is negligible, then in a conductance minimum W_1

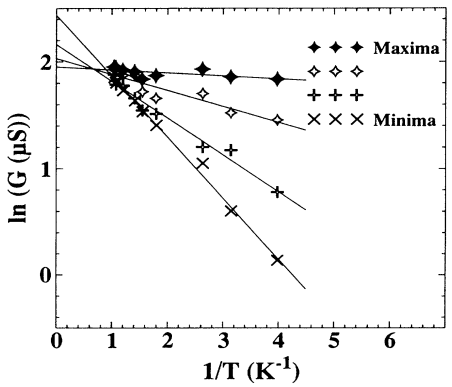

FIG. 3. Natural log of conductance vs $1/T$ with best fit straight lines, as measured on a peak, in a minimum, and at two points equally spaced in between.

$\approx W_2 \approx e^2/2C_\Sigma$. Figure 3 shows the Arrhenius plot [$\ln(G)$ vs $1/T$] of a conductance minimum: At temperatures > 250 mK this is a straight line. The slope gives an activation energy of 50 μeV and the intercept at $T=0$ is 11.4 μs. This activation energy is a factor of 5 smaller than the expected $e^2/2C_\Sigma = 250$ μeV. The intercept is almost exactly twice the low-temperature conductance measured on the adjacent peak (6 μs). Meirav *et al.* [6] also reported an activation energy 3.5 times less than expected from their estimate of C_Σ.

One explanation is that the levels are broadened by fluctuations of the dot potential caused by electron trapping close to the dot [14]. The width of the peaks measured at half the maximum does not change below ~ 200 mK. If this is caused by level broadening (and is not just the lowest temperature the electrons attain) then the activation energy should be reduced. The width of the peaks compared to the period at 200 mK suggests a reduction of the activation energy to ~ 100 μeV.

Another possible explanation is cotunneling; the dot minimizes its charging energy by emitting one electron at the far end of the device as an electron tunnels in the near side. The dot does not therefore charge up fully. The reduction in activation energy will then be given by the ratio of the tunneling time through one barrier to the RC time constant for the dot.

In conclusion, we have built a lateral quantum dot in close proximity to a separate circuit with a single constriction. This constriction is employed as a noninvasive voltage probe of the potential on the dot, which continues to work even after the conductance oscillations have become too small to be measured. The measured activation energy on a conductance minimum is much less than the expected value of half the charging energy.

We would like to acknowledge helpful discussions with Dr. C. J. B. Ford, Dr. M. C. Payne, and Dr. N. F. Johnson. This work was supported by the Science and Engineering Research Council and Esprit Project No. BRA6536.

[a]Also at Toshiba Cambridge Research Centre, 260 Cambridge Science Park, Milton Road, Cambridge CB4 4WE, United Kingdom.

[1] I. Giaever and H. R. Zeller, Phys. Rev. Lett. **20**, 1504 (1968); J. Lambe and R. C. Jaklevic, Phys. Rev. Lett. **22**, 1371 (1969).

[2] For a recent review, see D. V. Averin and K. K. Likharev, in *Mesoscopic Phenomena in Solids*, edited by B. L. Al'tshuler, P. A. Lee, and R. A. Webb (Elsevier, Amsterdam, 1991).

[3] P. Lafarge *et al.*, Z. Phys. B **85**, 327 (1991).

[4] T. J. Thornton *et al.*, Phys. Rev. Lett. **56**, 1198 (1986).

[5] For a review of CB effects in semiconductor devices, see H. van Houten, C. W. J. Beenakker, and A. A. M. Staring, in *Single Charge Tunneling*, edited by H. Grabert and M. M. Devoret, NATO ASI, Ser. B, Vol. 294 (Plenum, New York, 1992).

[6] U. Meirav *et al.*, Phys. Rev. Lett. **65**, 771 (1990).

[7] L. P. Kouwenhoven *et al.*, Z. Phys. B **85**, 367 (1991).

[8] C. G. Smith *et al.*, J. Phys. C **21**, L893 (1988).

[9] This possibility has been discussed by several theorists; see, e.g., R. Landauer, J. Phys. Condens. Matter **1**, 8099 (1989).

[10] Note that if the tunnel barriers were pinched off completely, to stop the connecting leads floating up to the applied potential, the size of the 2DEG region between the barriers would be much smaller than in the actual experiment, giving a much worse calibration.

[11] D. A. Wharam *et al.*, J. Phys. Condens. Matter **1**, 3369 (1989).

[12] B. J. van Wees *et al.*, Phys. Rev. Lett. **62**, 2523 (1989).

[13] R. J. Brown *et al.*, J. Phys. Condens. Matter **1**, 6291 (1989).

[14] D. H. Cobden *et al.*, Phys. Rev. B **44**, 1938 (1991).